BIOORGANIC CHEMISTRY 21, 439–475 (1993)

CONFERENCE PROCEEDINGS
Thirteenth Enzyme Mechanisms Conference

GORDON A. HAMILTON

Department of Chemistry, The Pennsylvania State University
University Park, Pennsylvania 16802

Received August 10, 1993

The Thirteenth Biennial Conference on Enzyme Mechanisms, organized by John A. Gerlt (Chair), Cynthia Burrows, Lawrence Marnett, Thomas Meek, and C. Dale Poulter, was held on January 6–9, 1993 at Key Largo, Florida. A total of 21 formal talks covering a broad array of topics in the general areas of enzyme mechanisms and bioorganic chemistry were given. In addition, two poster sessions were held with a total of over 100 posters being presented. In the following, a brief synopsis of each of the major talks, as well as a few select references to recent work in the area of the talk, are given. Also, the titles and authors of the posters are listed. It is hoped that this brief summary of the meeting not only will indicate the types of studies currently of interest to mechanism oriented bioorganic chemists, but also will serve as a starting point for those who wish to delve more deeply into the topics that were discussed.

1. HOW REVERSE TRANSCRIPTASE TRANSCRIBES

In the initial presentation Stephen J. Benkovic of the Pennsylvania State University described research he and his group have done to characterize various reactions catalyzed by reverse transcriptase. Retroviral reverse transcription, wherein single stranded viral RNA is converted into double-stranded proviral DNA, is catalyzed by the virally encoded enzyme reverse transcriptase (RT). This multifunctional enzyme can catalyze DNA-dependent and RNA-dependent DNA polymerization as well as the RNA hydrolysis of RNA · DNA hybrids (RNase H). The spatial and temporal relationship between the polymerase and RNase H activities of HIV-1 RT have been examined using a short RNA template and a series of DNA primers of lengths ranging from 15 to 40 nucleotides (*1*). Experiments where the catalytic events were limited to a single enzyme turnover indicate: (a) a spatial separation of 18 or 19 nucleotides between the polymerase and RNase H sites, and (b) that a tight temporal coupling exists between the two activities. The latter finding suggests that, while the polymerase and RNase H activities are distinct, both can occur concurrently.

During the course of reverse transcription, two DNA strand transfer reactions occur. The mechanism of minus strand strong-stop DNA transfer has been studied *in vitro* with HIV-1 RT and a model template–primer system derived from the HIV-1 RT genome (*2*). To accomplish strand transfer reactions, HIV-1 RT utilizes two kinetically distinct RNase H activities. The first, termed polymerase-dependent RNase H activity, cleaves the RNA template concomitantly with DNA syn-

0045-2068/93 $5.00

thesis. A second RNase H activity cleaves the remaining RNA fragments annealed to the nascent DNA strand prior to the transfer of DNA to the second RNA acceptor template. Kinetic and uv crosslinking experiments support a model where RT accommodates both the acceptor RNA template and the nascent DNA strand before the transfer event is completed. The polymerase activity of HIV-1 RT was found to incorporate additional bases beyond the 5′-end of RNA templates, resulting in a base misincorporation upon DNA strand transfer. Such a process occurring *in vivo* during homologous recombination could contribute to the hypermutability of the HIV-1 genome.

2. MICROGONOTROPENS AS AGENTS FOR DNA STRUCTURAL MODIFICATION

Thomas C. Bruice of the University of California at Santa Barbara summarized the research he and his group are pursuing with microgonotropens and their interaction with DNA. Microgonotropens are identified as designed agents which bind in the minor groove of DNA and which extend out of the minor groove in order to interact with phosphodiester linkages (to be able to catalyze hydrolysis) and/or the major groove (for recognition). The design rationale and synthesis, as well as the footprinting of the microgonotropens illustrated in Fig. 1 (namely *dien*-microgonotropens **5a**, **5b**, and **5c**, and *tren*-microgonotropens **6a** and **6b**), were discussed. Results from the use of a new fluorescent technique for the determination of the equilibrium constants for multiple binding of the microgonotropens to DNA were presented as well as the 2D ^{1}H NMR structure (Fig. 2) of the complex of **5c** with the double-stranded dodecamer CGCAAATTTGCG. Gel-shift studies suggest that the binding of microgonotropens (particularly **6b**) change the shape of the DNA oligomers

3. INTERCONVERSION OF CHEMICAL ENERGY AND WORK BY THE CALCIUM ATPASE OF SARCOPLASMIC RETICULUM

As pointed out by William P. Jencks of Brandeis University in his presentation, there are really two questions that need to be answered in order to understand how the chemical energy released in the hydrolysis of ATP is converted into the work that is performed in muscle contraction, active transport, and other coupled vectorial processes. An understanding of the processes requires that they must first be separated and then answered (*3–7*).

The coupling of ATP hydrolysis and the performance of work can be defined by a simple set of rules. These rules define specificities for: (a) catalysis of the hydrolysis of ATP to ADP and P_i in two or more steps, and (b) movement, which is also divided into two or more steps. The coupling of the chemical and vectorial processes arises simply from alternation of the chemical and vectorial steps so that neither the chemical nor the vectorial process can occur unless the other one

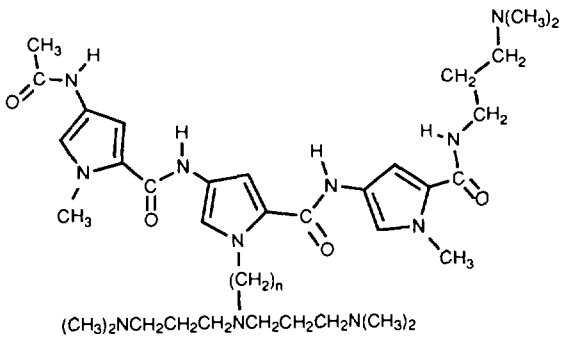

5a, n=3; **5b**, n=4; **5c**, n=5

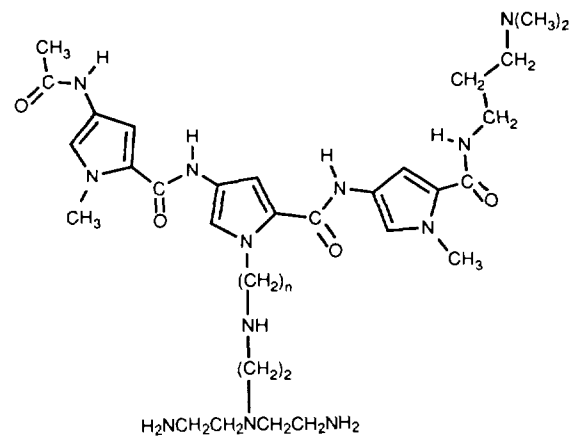

6a, n=3; **6b**, n=4

FIG. 1. Microgonotropen structures.

also occurs. This is illustrated for the reaction cycle of the calcium pump of sarcoplasmic reticulum by a simple four-step reaction cycle as shown in Fig. 3.

The second requirement is that the reaction must proceed at a useful rate; there must be no large thermodynamic or kinetic barriers along the reaction path. This requirement is met by the utilization of interaction energies that alter the Gibbs energies of intermediate species and transition states along the reaction path, so that there are no large barriers or deep wells in the Gibbs energy profile under physiological conditions. For example, it is found that the acyl phosphate intermediate in the reaction cycle of the calcium ATPase of sarcoplasmic reticulum is greatly stabilized relative to bound inorganic phosphate. In other work Dr. Jencks and his group have obtained evidence that the ATPase has two sets of sites for

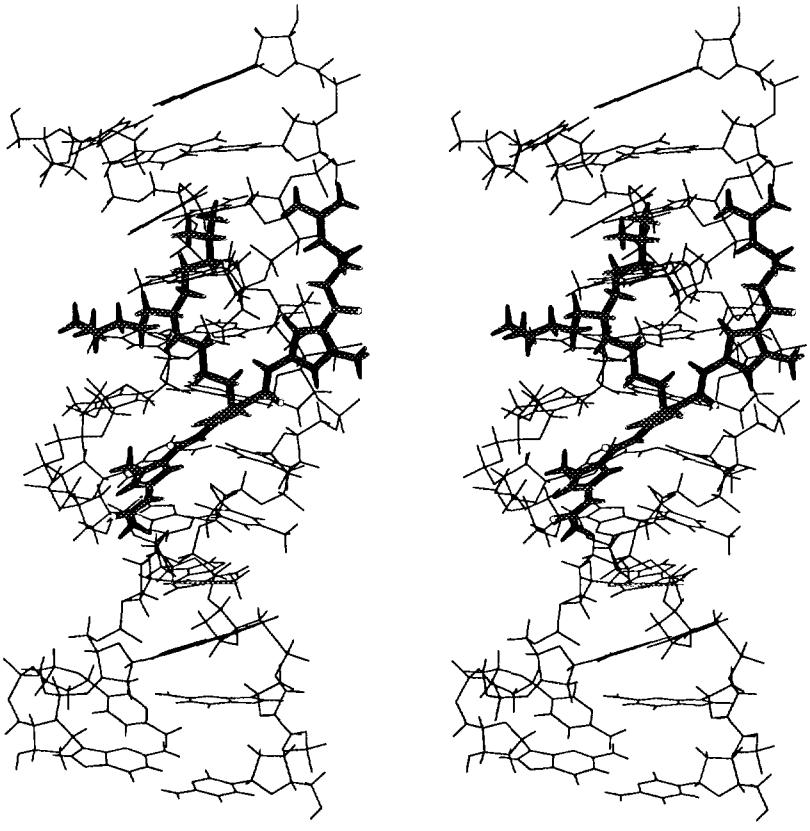

FIG. 2. Stereo view of **5c** complexed to a double-stranded DNA helix.

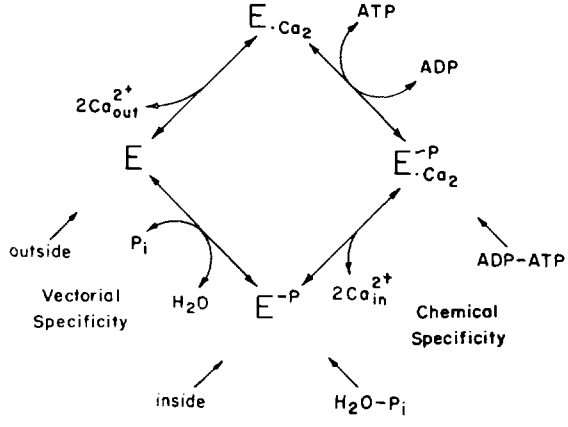

FIG. 3. Reaction cycle for the calcium pump of sarcoplasmic reticulum.

binding calcium, one internal and the other external and that phosphorylation shifts calcium from one to the other.

4. TRANSITION STATE STABILIZATION BY AN RNA CATALYST

Thomas R. Cech of the University of Colorado briefly summarized the history of RNA-catalyzed reactions and then focussed on some research he and his group are pursuing in attempts to understand how RNA carries such reactions out. The first catalytic RNA (ribozyme) identified was the self-splicing intron of the large subunit ribosomal RNA of the ciliated protozoan, *Tetrahymena thermophila*. This intron is a member of a phylogenetically diverse family called group I, which now consists of more than 100 sequenced examples. Shortened forms of the *Tetrahymena* intron catalyze the cleavage or ligation of exogenous RNA or DNA substrates with multiple turnover.

Measurement of the rate constants for the individual steps of ribozyme-catalyzed RNA cleavage has allowed evaluation of the quality of this catalyst. The chemical step occurs with a rate constant ($\sim$350 min^{-1}) that is $\sim 10^{11}$ times that estimated for uncatalyzed hydrolysis of RNA to give the same 5′-phosphate, 3′-hydroxyl reaction products (*8*). This is comparable to rate advantages achieved by protein enzymes. Furthermore, under $(k_{cat}/K_m)^S$ conditions the ribozyme cleaves the RNA substrate (S) as fast as it binds, and the rate constant for binding is similar to that measured for helix formation between two oligonucleotides. Because any improvement of the catalytic center would fail to increase $(k_{cat}/K_m)^S$, the ribozyme meets a limited definition of catalytic perfection (*8*).

How does an active site composed of RNA stabilize the transition state for RNA cleavage or RNA splicing? The current view of Dr. Cech and his co-workers (*9*) is summarized in Fig. 4. The guanosine nucleophile and the 3′-O leaving group have an in-line orientation, based on the determination of the stereochemical course of the reaction, inversion of configuration at phosphorus. The RNA substrate (CCCUCUAAAAA in Fig. 4) must be positioned next to the guanosine-binding site in the active site of the ribozyme, and this is accomplished through base pairing plus tertiary interactions (*10*). Some of the latter involve 2′-OH groups on the substrate strand (*11*).

All ribozymes require or are greatly stimulated by divalent metal ions, which in part contribute to proper folding of the catalyst. A direct role for the metal ion in active site chemistry is supported by a metal ion specificity switch (*12*). A nucleic acid substrate in which the 3′-oxygen atom at the cleavage site is changed to sulfur can no longer be cleaved in the presence of Mg^{2+} but is readily cleaved with added Mn^{2+}. Based on the known preference of Mg^{2+} vs Mn^{2+} for coordination by phosphate vs phosphorothioate, this result provides strong evidence for metal ion–3′-S(O) coordination stabilizing the developing negative charge on the leaving group (3′-O^- or S^-). Similar metal ion participation has been proposed by T. Steitz and co-workers for the 3′–5′ exonuclease activity of the Klenow fragment of DNA polymerase I.

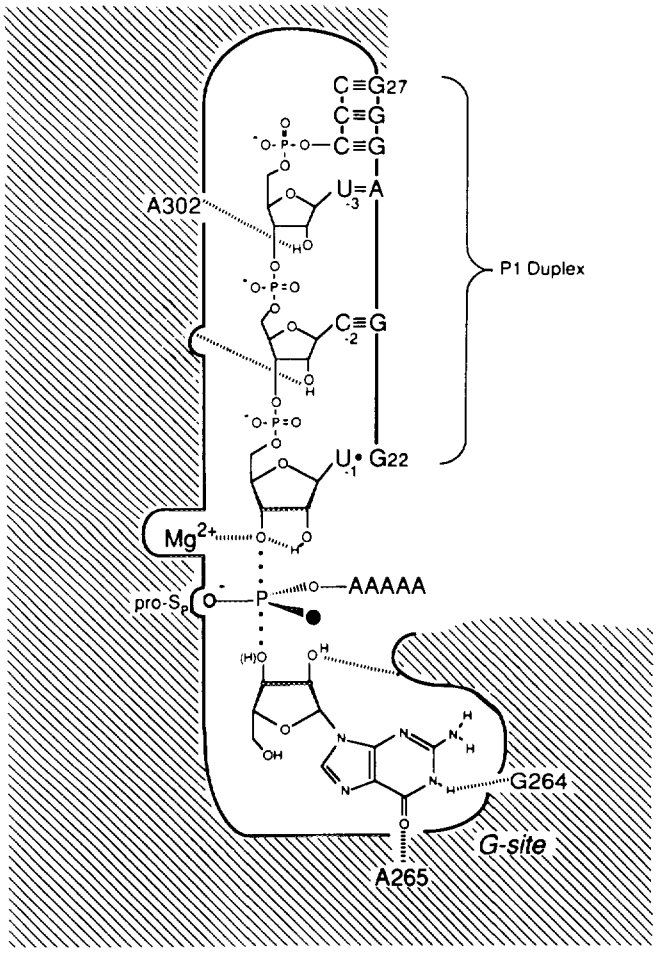

FIG. 4. Ribozyme–substrate interactions in the transition state (taken from Ref. *8*). The three-dimensional ribozyme surface is represented by the hatched pattern outside the dark outline; dashed lines, H-bonds or metal ion–oxygen coordination; dotted P–O bonds, bonds partially formed or partially broken in the transition state; shaded oxygen atom, *pro*-R_p oxygen.

5. CHEMICAL AND ENZYMATIC KETONIZATION OF DIENOLS IN MICROBIAL PATHWAYS

Recent investigations in this area were summarized by Christian P. Whitman of the University of Texas at Austin. The conjugated enol, 2-hydroxymuconate (**1**, Fig. 5), is an unusually stable dienol generated in the course of the bacterial catabolism of catechol by the enzymes of the meta-fission pathway. The dienol ketonizes chemically in aqueous solution or enzymatically by the action of 4-oxalocrotonate tautomerase (4-OT). In aqueous phosphate buffer a rapid interconversion of **1** and **2** before a much slower conversion to **3** (Fig. 5) is observed (*13*).

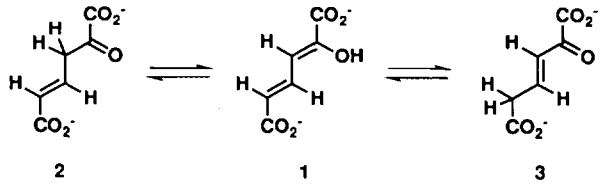

2 1 3

FIG. 5. Keto–enol interconversions involving the conjugated enol 2-hydroxymuconate (**1**).

Its non-enzymatic properties are fully consistent with the properties observed for other so-called slow-reacting dienols (*14*). The rapid interconversion of **1** and **2** raises the question of whether the enzyme utilizes **1** or **2** as its substrate. The values of k_{cat}/K_m determined for **1** and a mixture of **1** and **2** indicate that 4-OT is an efficient catalyst processing either isomer near the diffusion control limit. A reasonable hypothesis to explain these observations is that 4-OT is an isomerase catalyzing the transformation of **2** to **3** through the intermediacy of **1** (*13*).

In order to further address mechanistic and structural questions, the *xylH* gene encoding 4-OT was located and inserted into an *Escherichia coli* expression vector. By utilizing the *E. coli* alkaline phosphatase promoter (*phoA*), Dr. Whitman and his co-workers were able to express functional 4-OT in yields of at least 10 mg of pure enzyme/liter of culture. The functional unit is apparently a pentamer of identical subunits, each consisting of only 62 amino acid residues. The amino acid sequence does not show homology with any of the sequences in the current data bases nor with any of the sequences of enzymes that catalyze similar reactions (*15*).

Considerable mechanistic insight into the 4-OT reaction can be obtained by determining whether the 1,3-proton transfer is a suprafacial or an antarafacial process. A straightforward approach to this question is complicated by the fact that **2** has not been synthesized or isolated; it can only be detected in rapid equilibrium with **1**. Dr. Whitman's strategy, therefore, was based on the expected enzyme partitioning of **1** to [3-$^2H_1$]**2** and [5-$^2H_1$]**3** in ^2H_2O.

The stereochemistry of [5-$^2H_1$]**3** was examined first. In ^2H_2O, in the presence of 4-OT, ketonization of **1** generates [5-$^2H_1$]**3**. The product was trapped by reduction with $NaBH_4$ and processed to [2-$^2H_1$]glutaric acid by chemical degradative procedures. The configuration was established by comparing the molar ellipticity of the isolated glutaric acid to that of a sample generated by a stereoselective synthesis. It was concluded that 4-OT ketonizes **1** stereospecifically to (5*S*)-[5-$^2H_1$]**3** (*16*). The analysis of the stereochemistry of [3-$^2H_1$]**2** was precluded by two observations. It is unknown at what time interval the maximal amount of [3-$^2H_1$]**2** is present and [3-$^2H_1$]**2** rapidly enolizes to [3-$^2H_1$]**1** resulting in a considerable loss of stereospecifically labeled compound.

An alternate strategy was devised based on the observed nonenzymatic and enzymatic properties of 2-hydroxy-2,4-pentadienoate (**4**, Fig. 6). In aqueous buffer, **4** ketonizes to **5** (Fig. 6) before a much slower conversion to **6**. 4-OT accelerates the rate of formation of **5** and **6**. However, **5** is generated by 4-OT at a significantly higher rate than is **6**. This observation coupled with the fact that **5** accumulates

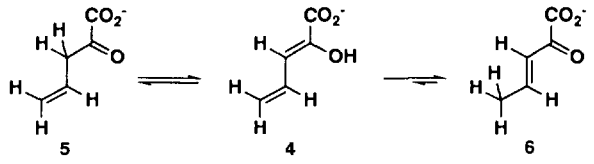

FIG. 6. Enzymatic and nonenzymatic ketonizations of 2-hydroxy-2,4-pentadienoate (**4**).

in solution suggested that the ketonization of **4** to **5** could be used to assign the stereochemical course of 4-OT. Accordingly, [3-^{2}H]**5** was generated by the 4-OT-catalyzed ketonization of **4** in ^2H_2O; the product was reduced by $NaBH_4$, processed to malate by ozonolysis, and analyzed by ^{1}H NMR. This analysis showed a predominance of deuterium in the (3*S*) position of malate indicating that 4-OT ketonizes **4** stereospecifically to (3*R*)-[3-^{2}H]**5** (note the change in priority numbering). This result and the stereochemical outcome above demonstrates that the isomerization of **3** to **2** is a syn process indicative of a one base mechanism (*17*).

6. STEROID ISOMERASE: MODELS, MECHANISM, AND MUTANTS

In his presentation Ralph M. Pollack of the University of Maryland, Baltimore County, described his research concerning 3-oxo-Δ^5-steroid isomerase (also known as Δ^5-3-ketosteroid isomerase, KSI) which catalyzes the isomerization of a variety of 3-oxo-Δ^5-steroids to their conjugated Δ^4-isomers through a dienol(ate) intermediate. The generally accepted mechanism for this reaction involves abstraction of the C-4β proton by the carboxylate of aspartic acid-38, with concomitant electrophilic catalysis (probably hydrogen bonding) by the hydroxyl group of tyrosine-14 to give a dienol intermediate. This intermediate is then protonated at C-6β by the conjugate acid of aspartic acid-38 (Fig. 7).

Free energy profiles were determined for the acetate-ion-catalyzed isomerization of 5-androstene-3,17-dione (R = O) as a model system for the KSI-catalyzed reaction (*18*). The free energy profile of the KSI-catalyzed reaction was obtained from a combination of steady-state kinetic parameters in water and deuterium oxide and the observed partitioning of the dienol intermediate when it is treated with the enzyme (*19*, *20*). The free energy profile of the enzymatic reaction reveals

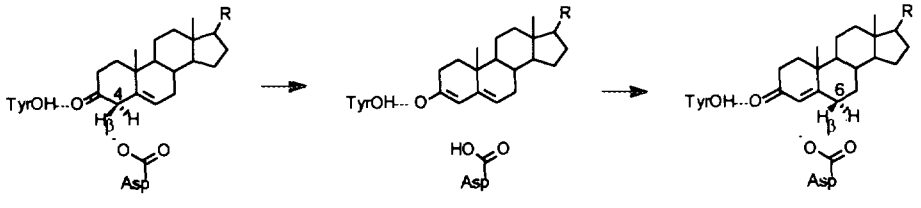

FIG. 7. Mechanism for the reaction catalyzed by Δ^5-3-ketosteroid isomerase.

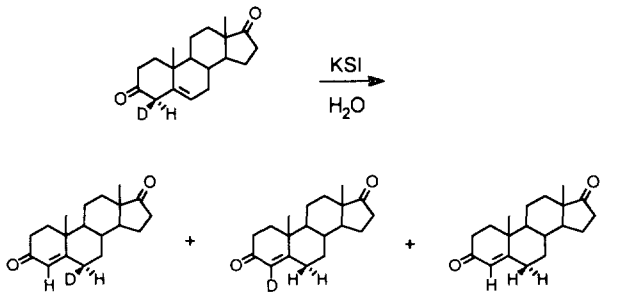

WT	47 %	24 %	29 %
D38E	9 %	66 %	25 %

FIG. 8. Products formed with wild type and mutant Δ^5-3-ketosteroid isomerases.

that the internal equilibrium constant for the substrate–dienol equilibrium is perturbed from its value in solution (1/500) to near unity. The relative energies of the transition states for diffusion of enzyme and substrate, for deprotonation and for protonation of the intermediate, are similar. A comparison of the free energy profiles for the enzymatic reaction and the model reactions allows the catalysis to be dissected into a combination of (a) uniform binding of the steroid due to the hydrophobic active site; (b) differential binding of the intermediate dienol and the transition states leading to/from it by tyrosine-14; and (c) catalysis of proton transfer by aspartic acid-38.

A mutant enzyme in which the active site aspartic acid is replaced by a glutamic acid (D38E) shows a decreased value of k_{cat} (300-fold) and of k_{cat}/K_m (165-fold) toward 5-androstene-3,17-dione (R = O). Toward 5-pregnene-3,20-dione (R = $COCH_3$) smaller decreases in k_{cat} (32-fold) and k_{cat}/K_m (25-fold) are observed (*21*). Product studies (Fig. 8) and kinetic isotope effect measurements show that the D38E mutant preferentially abstracts the 4α proton from 5-androstene-3,17-dione during catalysis, in contrast to the wild-type KSI, which preferentially abstracts the 4β proton (*22*).

7. SPECTROSCOPIC AND MECHANISTIC PROBES OF CROTONASE: IS THERE AN ENOL(ATE) INTERMEDIATE?

As summarized by Vernon Anderson of Case Western Reserve University in his presentation, isotope effects on the crotonase-catalyzed elimination of the pro-2R hydrogen and 3-hydroxyl from 3-hydroxyacyl-pantetheine substrates have been interpreted as being consistent with a concerted reaction (*23, 24*). The main observation was that the presence of deuterium at the primary position left the α-secondary deuterium isotope effect, which reports on hybridization changes at the hydroxyl-substituted carbon, unchanged. This conclusion is at odds with the

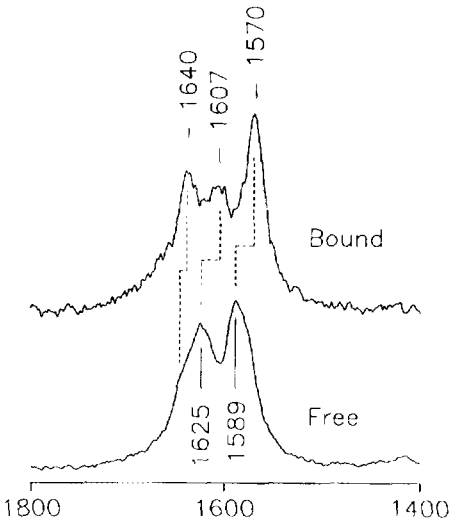

FIG. 9. Resonance Raman spectra of hexadienoyl-CoA both free and bound to crotonase.

more common stepwise elimination mechanism with an enol(ate) intermediate, long presumed to be present because of the uv absorption spectra of crotonase bound acetoacetyl-CoA.

The effect of pH on V/K for crotonyl-CoA revealed no catalytically active functional groups in the pH range from 3.9 to 10.0. The inhibition constant for *trans,trans*-2,4-hexadienoyl-CoA was invariant with pH while that for acetoacetyl-CoA increased at both low and high pH. The increasing K_i for acetoacetyl-CoA at high pH is inconsistent with the enolate form being the true inhibitor. Resonance Raman (RR) studies (324 nm illumination) showed dramatic differences between the enzyme bound form of the inhibitor and the enolate generated either by ionization at high pH or by addition of Mg(II), indicating the nature of the interaction of the acetoacetyl moiety with the active site cannot be inferred from the uv spectra alone.

When hexadienoyl-CoA (HD-CoA) binds to crotonase, the uv absorption λ_{max} increases from 296 to 320 nm. This is inconsistent with protonation of the carbonyl which yields a maximum absorption near 390 nm. The vibrational character of the conjugated chromophore was investigated with RR spectroscopy of the free and bound HD-CoA. Three bands in the 1590–1650 cm^{-1} region can be detected in both the free and bound species (Fig. 9). The association red-shifts the two lower frequency bands by about 18 cm^{-1}. These two bands were identified as being derived largely from the conjugated carbonyl and C2–C3 stretch by substitution of ^{18}O and ^{13}C at the carbonyl and C-2 positions, respectively. The polarization of the carbonyl in the product is indicative of electrophilic catalysis, but the magnitude of the alkene polarization cannot be adequately explained solely by H-bonding to the carbonyl. A similar situation occurs in the ketosteroid isomerase system (*25*).

When *para*-substituted cinnamoyl-CoAs were bound to crotonase the λ_{max} of

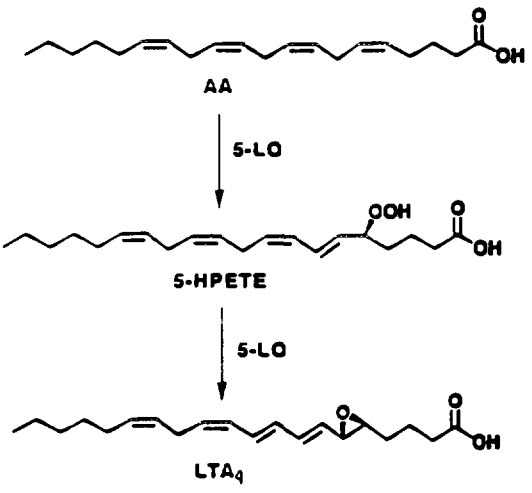

FIG. 10. Two of the reactions catalyzed by 5-lipoxygenase.

the bound CoA thioesters were similarly red-shifted, a minimum of 8 nm with the *para*-nitrocinnamoyl-CoA to 90 nm with *para*-dimethylaminocinnamoyl-CoA. A correlation of the dissociation constants with Taft σ^+ constants revealed a positive correlation with a slope of near one for the electron donating cinnamoyl-CoAs. The electron withdrawing *para* substituents, chloro and nitro, led to smaller dissociation constants as well, suggesting that both polarization of the carbonyl through resonance electron donation as well as inductive electron withdrawal from C-3 lead to enhanced affinity for the active site. Thus polarization of the alkene and carbonyl were detected both by RR spectroscopy and by the binding of the cinnamoyl-CoAs. These interactions will both increase the acidity of the α-proton abstracted in the reaction and lower the kinetic barrier for Michael addition. The carbonyl activation leads to the stereospecific exchange of the pro-2S proton of butyryl and octanoyl-CoA. However, besides being the opposite stereochemistry from the elimination reaction, the exchange reaction has a sharp pH maximum and is over 1000-fold slower than the elimination reaction, indicating it is not necessarily relevant to the physiological reaction (*26*).

8. 5-LIPOXYGENASE: CATALYTIC MECHANISM AND INHIBITION

In his presentation Michael J. Gresser of Merck Frosst Canada summarized extensive information on human leukocyte 5-lipoxygenase (5-LO), which catalyzes the oxygenation of arachidonic acid to 5-HPETE and LTA_4 as shown in Fig. 10 (*27*). In the absence of oxygen the enzyme catalyzes the reduction of fatty acid hydroperoxides by arachidonic acid, and by reducing agents such as *N*-hydroxyureas and catechols in the presence or absence of oxygen. A mechanism accounting

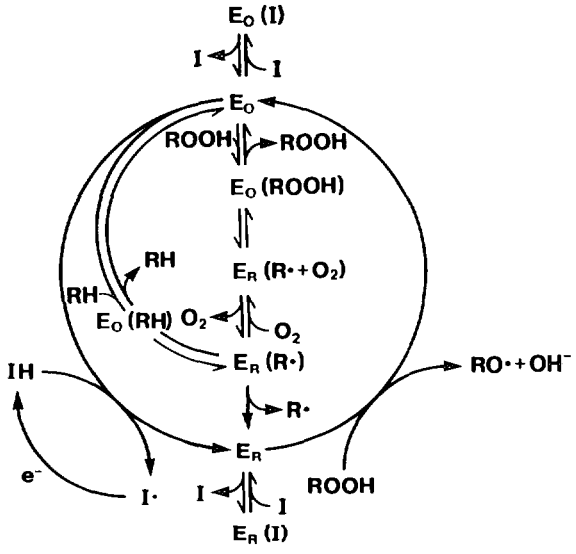

FIG. 11. A kinetic mechanism for the activities of 5-lipoxygenase, and its inhibition by reducing agents and by reversible dead end inhibitors. E_O and E_R represent the oxidized and reduced forms of the enzyme, respectively, which can reversibly bind dead end inhibitors, I. Reducing inhibitors and their one electron oxidized products are represented by IH and I$^{\cdot}$, respectively. The substrate, arachidonic acid, is represented by RH, and R$^{\cdot}$ is the pentadienyl radical intermediate. The product 5-HPETE is represented by ROOH, which can also react with E_R to yield E_O, hydroxide anion, and an alkoxy radical. The radical generating processes are represented as irreversible, and the binding steps for IH and ROOH to E_O and E_R, respectively, are not shown explicitly in the scheme.

for these activities is shown in Fig. 11 (*28*). The redox center is a nonheme iron and site directed mutagenesis studies have shown that at least two conserved histidine residues are essential for full oxygenase activity; one of them is essential for iron binding (*29*). Aerobic inactivation has been found to be caused by H_2O_2 reacting with the reduced form of the enzyme (*30*). Reducing agents inhibit the oxygenase activity by acting as alternative substrates in a redox cycle involving fatty acid hydroperoxide. Reversible dead end inhibitors inhibit both the oxygenase and redox cycle activities and protect 5-LO from turnover inactivation as well (*31*). Some of the reversible dead end inhibitors appear to interact selectively with the reduced form of 5-LO, as indicated by their decreased potency in the presence of fatty acid hydroperoxides and potentiation of their inhibition by reducing agents. Most reversible dead end 5-LO inhibitors discovered thus far are relatively insensitive to the presence of either reducing agents or fatty acid hydroperoxides. These inhibitors are considered to bind with roughly equal affinity to either oxidized or reduced 5-LO, as shown in Fig. 11.

9. MECHANISM OF PYRUVATE FORMATE LYASE AND ITS ACTIVATION

As summarized in the presentation by John W. Kosarich, formerly of the University of Maryland, College Park, this enzyme (*32, 33*), which catalyzes the reversible

interconversion of pyruvate and CoASH to formate and acetyl-CoA, has an organic radical (thought to be a peptidyl glycyl radical), is very sensitive to oxygen and is activated by anaerobiosis. Furthermore, an enzyme that catalyzes the activation of the lyase requires *S*-adenosylmethionine for activity. In mechanistic studies Dr. Kosarich and his group have obtained evidence that the lyase functions by catalyzing two half reactions, one being the reaction of pyruvate with an enzymic thiol group to give formate and an acetyl thioester form of the enzyme, and the second being the transfer of the acetyl group from the enzyme to CoASH to give acetyl-CoA and regenerate the free enzyme. The first half reaction presumably occurs by a radical reaction and some possibilities were considered.

10. MECHANISM OF HYDROCARBON ACTIVATION BY METHANE MONOOXYGENASE

John D. Lipscomb of the University of Minnesota summarized the extensive work that he and his co-workers have done with this enzyme (*34–38*). The soluble form of methane monooxygenase (MMO) isolated from *Methylosinus trichosporium* OB3b consists of three protein components: hydroxylase (MMOH), with an $\alpha_2\beta_2\gamma_2$ subunit structure containing two μ-(R/H)oxo-bridged dinuclear iron clusters; reductase; containing an FAD and a [Fe_2–S_2] cluster; and component B, containing no cofactors. The enzyme catalyzes oxidation of an exceptionally wide range of compounds including linear, branched, cyclic, aromatic, heterocyclic, and halogenated hydrocarbons. In past experiments, Dr. Lipscomb and his group have shown that the hydroxylase component alone can catalyze monooxygenase chemistry if it is first nonenzymatically reduced to the two electron reduced state and then exposed to O_2 and substrate. A single turnover ensues to generate the same products as the reconstituted three component system coupled to NADH oxidation. Based on this observation and the general similarity of the reaction to that of cytochrome P450, the mechanism for catalysis shown in Fig. 12 was proposed. In this mechanism, the diiron cluster is reduced to the two electron reduced state and then reacts with O_2. Heterolytic cleavage of the O_2 bond results in production of water and the activated form of oxygen bound to the enzyme. The latter species is proposed to be an oxygen atom bound to the diiron cluster. In the [Fe(IV) · Fe(IV)] resonance form, the cluster could provide two electrons to the oxygen atom to stabilize it by completing its valence octet. By analogy with cytochrome P450 one resonance form of this species could abstract a hydrogen atom from the substrate to give a substrate radical and a hydroxyl bound to the [Fe(IV) · Fe(III)] cluster. Rebound chemistry would give the product and regenerate the oxidized cluster.

In his presentation Dr. Lipscomb presented considerable chemical and kinetic evidence supporting this cycle. The mechanism implies that the two reducing equivalents and the oxygen needed for catalysis might be supplied together in the form of H_2O_2. This "peroxide shunt" has now been shown to function so that in the presence of H_2O_2 the oxidized MMOH can catalyze the characteristic MMO chemistry anaerobically and without a biological or nonbiological reducing source.

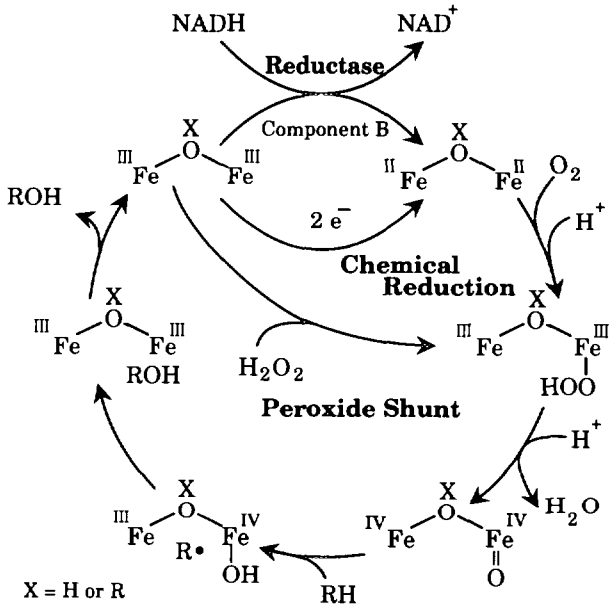

FIG. 12. Proposed catalytic cycle of methane monooxygenase.

The catalytic cycle also implies the formation of an intermediate substrate radical. This was tested by oxidizing chiral (*R*) or (*S*) 1-(^{1}H,^{2}H,^{3}H)ethane in an MMO-catalyzed reaction. The configuration of the resulting ethanol from either the NADH- or H_2O_2-coupled reaction was shown by tritium NMR to be 35% inverted relative to that of the starting stereoisomer; this implies the formation of a substrate intermediate that can flip before completion of the reaction. The extent of inversion indicates that the substrate intermediate must not be bound in a specific orientation in the active site, but it also cannot diffuse out of the active site before the reaction is complete. An ethyl radical is the favored intermediate based on energetic arguments.

Kinetic experiments were also reported that indicate the formation of two transient intermediates of the reaction cycle and imply the formation of at least two others. Freeze quench EPR studies show that the fully reduced hydroxylase in the presence of component B reacts with O_2, at least 40-fold faster than the maximal turnover number, to form an EPR silent and colorless intermediate. This intermediate is converted in a slower reaction to a new chromophoric intermediate (compound Q) with a λ_{max} at approximately 430 nm. Optical and chemical quench studies show that compound Q is converted to the enzyme–product complex at a substrate-concentration-dependent rate. The enzyme–product complex decays to free enzyme and product in the rate limiting step of the reaction. No EPR spectrum is observed during the process of compound Q decay; thus the intermediate substrate radical probably forms and decays rapidly as implied by the extent of inversion observed in the chiral ethane experiment. Since compound Q can be

formed with or without substrate, but decays in a manner that depends on both the type and the concentration of substrate, it may be a form of the enzyme containing the reactive oxygen species or one leading directly to its formation. These results are in accord with the number and nature of the intermediates depicted in the proposed reaction cycle.

11. FROM MODEL ENZYMES TO MODEL MEMBRANES

John T. Groves of Princeton University described some of the recent research he and his group have done developing membrane soluble catalysts that oxidize various lipid components at specific sites (*39*). The catalysts are various porphyrin derivatives that have extensive hydrocarbon groups attached, thus making the catalysts soluble in membranes and imparting specificity to the oxidation of membrane components.

12. INACTIVATION OF COBALAMIN-DEPENDENT METHIONINE SYNTHASE BY N_2O: DEATH BY LAUGHING

As pointed out in the presentation by Rowena G. Matthews of the University of Michigan, methionine synthase, which catalyzes the reaction of *N*-methyltetrahydrofolate with homocysteine to give tetrahydrofolate and methionine (*40*), is especially important in one carbon metabolism, and thus affects, among others, the biosynthesis of purines and pyrimidines. The holoenzyme of about 137 kDa can be cleaved into several domains, including a 29-kDa cobalamin-binding domain whose X-ray structure is now being determined (*41*) and a C-terminal *S*-adenosylmethionine-binding domain of 37 kDa. When the enzyme is inactivated by oxidation, it needs SAM as well as a reducing agent to be reactivated. Dr. Matthews believes that the inactivation of methionine synthase by N_2O is due to the formation of the hydroxyl radical, which then attacks some enzymic group. Characterization of the exact mechanism of inactivation is still being pursued.

13. BIOSYNTHESIS OF 3,6-DIDEOXYHEXOSES

Hung-wen (Ben) Liu of the University of Minnesota summarized research that he and his group are doing on this topic. The 3,6-dideoxyhexoses are found in the lipopolysaccharide of gram-negative bacteria where they have been shown to be dominant antigenic determinants. They are synthesized via a complex series of enzymatic reactions starting, in most cases, from CDP-D-glucose. The first step is an irreversible intramolecular oxidation–reduction catalyzed by an NAD^+-dependent CDP-D-glucose 4,6-dehydratase (E_{od}). The nascent product, CDP-4-keto-6-deoxy-D-glucose, is then converted to CDP-4-keto-3,6-dideoxy-D-glucose in two consecutive enzymatic reactions mediated by CDP-4-keto-6-deoxy-D-glucose-3-dehydrase (E_1), a pyridoxamine phosphate (PMP) linked enzyme, and CDP-

6-deoxy-D-3,4-glucoseen reductase (E_3), an NADH-dependent catalyst, both of which had been purified from *Pasturella pseudotuberculosis*. Although the catalytic roles of these enzymes have been well defined, their intimate mechanisms is still disputable (*42*). In an effort to clarify these mechanistic ambiguities, Dr. Liu and his co-workers have isolated the CDP-D-glucose pyrophosphorylase, CDP-D-glucose 4,6-dehydratase, and an E_1 as well as an E_3 equivalent from a different bacterial strain *Yersinia pseudotuberculosis* (*43–45*). To further our mechanistic understanding of ascarylose production, they have recently cloned and characterized the gene cluster encoding the proteins of this important biosynthetic pathway. This represents the first example of the complete characterization correlation of gene products with their catalytic activities for an entire 3,6-dideoxyhexose pathway, providing distinct molecular evidence supporting the postulated sequence of events not only in the biosynthesis of ascarylose, but also the formation of other 3,6-dideoxyhexoses.

The chemical and catalytic properties of the purified E_1 and E_3 have been studied in detail. While E_3 is found to be a flavoprotein containing one plant-type ferredoxin [2Fe–2S] center (*46*), study of E_1 reveals that it is PMP dependent and also contains one plant-type ferredoxin [2Fe–2S] cluster. As apo-[2Fe–2S] forms of both E_1 and E_3 showed no sugar reductase activity, the iron–sulfur centers must play essential roles in the electron transfer from E_3 via E_1 to the glucoseen intermediate (the E_1 product). The order of electron flow has now been established as NADH–FAD–[2Fe–2S] of E_3—[2Fe–2S] of E_1—E_1 bound glucoseen intermediate. Based on the physical and chemical characteristics of E_1 and E_3, several possible mechanisms of their catalyses are proposed. The occurrence of a radical intermediate during E_1/E_3 catalysis is supported by the observation of a free radical signal at $g = 2.013$ in EPR analysis. The radical nature of this C-3 deoxygenation is reminiscent of the well-known sugar deoxygenation catalyzed by ribonucleotide reductase, albeit the mechanisms of these two deoxygenations are fundamentally distinct. The insights gained from these studies provide compelling evidence suggesting a biological deoxygenation is effected by a new and novel radical process.

14. ENZYME CHEMISTRY IN HISTIDINE BIOSYNTHESIS

As pointed out in the presentation by V. Jo Davisson of Purdue University, the biosynthesis of histidine is unique to plants and microorganisms and represents an intense expenditure of metabolic energy requiring the hydrolysis of five high energy phosphate bonds, a carbon and nitrogen atom from ATP, and a ribose unit to assemble a single amino acid molecule. For these reasons, investigations of the regulatory events in this pathway have been of central importance and have resulted in a wealth of genetic information (*47*). A diverse array of enzymatic transformations is represented in the pathway; however, a limited knowledge base exists regarding the proteins and their associated mechanisms (*48, 49*). At this juncture the interests of Dr. Davisson and co-workers have focused upon the isolation and characterization of the constituent proteins using a series of over producing strains of *Escherichia coli* that have been prepared in their laboratory.

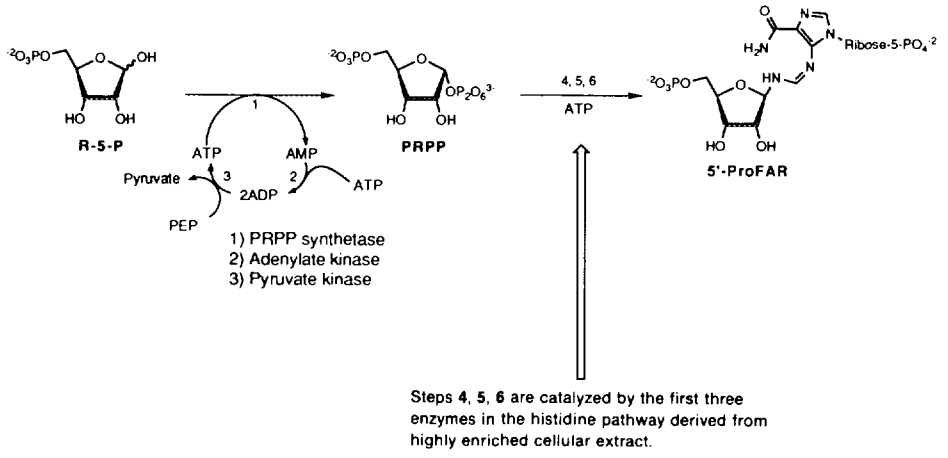

FIG. 13. Strategy for the preparation of histidine biosynthetic intermediates.

Individual plasmid constructs for eight of the histidine biosynthetic genes have been prepared which direct the regulated overexpression of the respective proteins. A second series of plasmid constructs have also been prepared that contain multiple biosynthetic genes under the control of a single RNA polymerase (*tac*) promoter and that direct the high level expression of the desired enzymes involved in sequential steps in the histidine pathway. Crude protein extracts from *E. coli* cells harboring these tailored "mini-operon" constructs have been used in the direct enzymatic syntheses of key pathway intermediates such as N^1-(5″-phospho-β-D-ribosyl)-formimino-5-aminoimidazole-4-carboxamide ribonucleotide (5′-ProFAR). A simple *in situ* enzymatic system for the generation of PRPP has been coupled with the histidine enzyme extracts to allow these syntheses (Fig. 13) to be executed on a mmole scale from ribose-5-phosphate. The structures of the intermediates have been established by modern spectroscopic techniques. With these compounds in hand, *in vitro* studies of the constituent enzymes can now proceed.

Attention has recently been focused on the enzymology of imidazole ring formation in a central step of the pathway, the transformation of the nucleotide substrate N^1-(5″-phospho-β-D-ribulosyl)-formimino-5-aminoimidazole-4-carboxamide ribonucleotide (PRFAR) to imidazole glycerol phosphate (IGP) and 5′-(5-aminoimidazole-4-carboxamide) ribonucleotide (AICAR) (Fig. 14). In *E. coli*, there are two genes *hisH* and *hisF* that are associated with this process. The nature of the catalytic activities of each of these proteins had not been established and several hypotheses existed for a possible intermediate in the pathway (*47, 50*). The source of nitrogen for the ring formation had been postulated to be glutamine. By amino acid sequence comparison, it was discovered that the *hisH* protein had a high degree of sequence identity with the active site regions of the *trpG*-type subclass of glutamine amidotransferases and includes a putative Cys–His–Glu catalytic triad found in these proteins (*51*). Homogenous preparations of the *hisH* and *hisF*

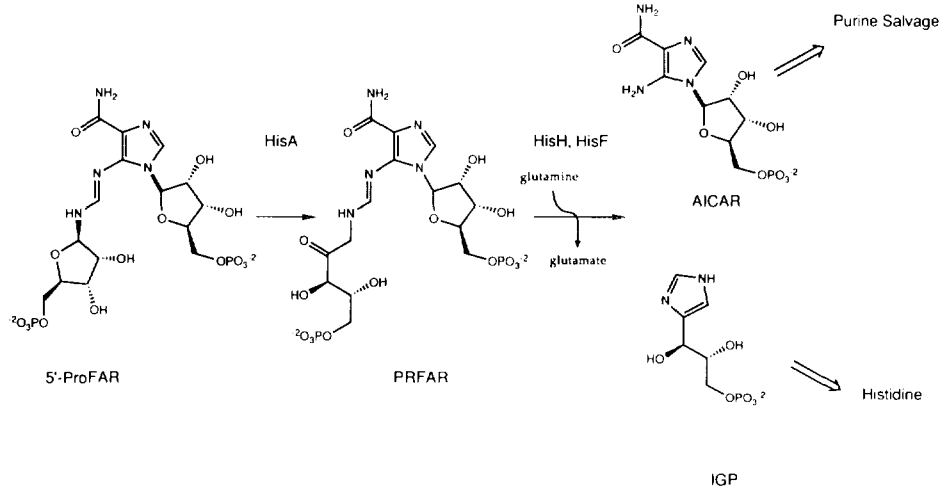

FIG. 14. Some steps in the biosynthesis of histidine.

proteins displayed glutamine-dependent activity only when both proteins were included in the assay. Under the conditions of the experiments, it was concluded that no free intermediate occurs in the pathway. These results led to a series of experiments which allowed the isolation and characterization of an $\alpha\beta$ dimeric holoenzyme consisting of the *hisH* and *hisF* proteins. This has been named IGP synthase. A remarkable series of activities are displayed by this enzyme and include a glutamine amidotransferase, carbon–nitrogen cycloligase, and carbon–nitrogen lyase. Despite the capacity for the *hisF* protein alone to behave as IGP synthase with NH_4Cl as a nitrogen donor, the studies indicate that glutamine is the most efficient substrate. Although the *hisH* protein has no inherent catalytic activity, when bound to the *hisF* protein this subunit is responsible for the amide transfer reaction. These results constitute the first biochemical evidence that corroborates previous genetic studies indicating an essential role for both of these proteins in the *de novo* biosynthesis of histidine.

In the course of establishing the stoichiometry of the reaction catalyzed by IGP synthase, a glutaminase activity was detected in the presence of the product IGP after complete consumption of the nucleotide substrate. This 50-fold stimulation of k_{cat} was specific for IGP; the second product AICAR had no effect on glutaminase activity. The biosynthetic precursor for the nucleotide substrate 5'-ProFAR also demonstrated this property and appeared to be a substrate analog. The influence of substrate and product binding to the *hisF* domain as they relate to the catalytic properties of the *hisH* protein were also studied with the glutamine antagonist 6-diazo-5-oxonorleucine (DON). This irreversible inhibitor has similar effects on other glutamine amidotransferases and effects a sulfhydryl alkylation event at the active site cysteine residue (*51*). In the presence if IGP, 5'-ProFAR, or PRFAR, the rate of irreversible inactivation by DON was the only step influenced by the